International Journal of Engineering Research & Technology (IJERT)
ISSN: 2278-0181
Vol. 9 Issue 12, December-2020

Quasi-Mechanistic Analyses of Impact of Vibrational Dynamic Loading on Characteristics of Clayey and Gravelly Geomaterials

John Ngaya Mukabi
R&D/Design Dept.
Kensetsu Kaihatsu Consulting Engineers Ltd.
Nairobi, Kenya

Abstract **— A desirably realistic modelling and simulation approach for pavement and related geo-structures is to effectively replicate the effects of vibrational dynamic loading (VDL), which is the prevalent mode of loading on practically all live load-imposed structures. In this Study, an innovative comprehensive testing regime was designed to simulate the vibrational dynamic loading commonly experienced during in-service of highway and airport pavements. Based on experimental test results simulating a variety of testing and loading conditions adopted for varying geomaterials, sophisticated analytical models, introduced in this paper, were developed. The validity, lucidity and rationality of the proposed TACH-MD VDL analytical models is pragmatically demonstrated through comparison with experimental testing results. Effective application of these models in the design of highway and airport pavements is ascertained based on tabulated results, graphical plots and analytical discussions. It is rationally derived that the proposed TACH-MD VDL analytical models can be effectively applied for natural and hydraulically stabilized clayey and gravelly geomaterials as well as unbound and bound crushed stone aggregates.**

Keywords — Vibrational dynamic loading, VDL, analysis, analytical models, quasi-mechanistic, clayey, gravelly, geomaterial.

I. INTRODUCTION

The application of effective quasi-empirical and analytical models that can facilitate for the precise analysis and structural evaluation of the effects of vibrational dynamic loading is indeed one of the most fundamental prerequisites in pavement engineering. In this Study, TACH-MD VDL analytical models that can simulate and account for the effects of vibrational dynamic loading commonly experienced during in-service of highway and airport pavements, are introduced as part of essential design tools [1].

Furthermore, consideration of the fact that some pavements will certainly not be subjected to high intensity dynamic loading, it is imperative that a more realistic approach based on a multi-stage loading regime that takes into account a rebound effect due to post-dynamic-static loading stress release, has been made accordingly. Consequently, a number of tests under sustained dynamic loading to simulate critical state conditions and consideration of future increase in load intensity were performed for this sake [1]. It is important to note that the Airports that can be appropriately characterized with due reference to the sustained dynamic loading model are the likes of Heathrow and JF Kennedy which have landings and take-offs every other minute [1]. Based on the foregoing considerations therefore, several modes of loading including sustained and multi-stage loadings were meticulously designed and carried out on specimens that represent typical pavement and subgrade materials as well as structural layer configurations in due consideration of the intensity and direction of the impacted stresses [1]. The reliability and effectiveness of applying the proposed models is explicitly manifested in this paper whereby explicable discussions are made in retrospect to the pragmatic pavement structural design of aerodromes in Kenya and Somalia.

II. CORE TACH-MD MODELS FOR DERIVING SHEAR AND MAXIMUM IMPACT STRESSES

Rutting is one of the most important load-induced distresses frequently encountered in flexible asphalt pavements. The primary mechanism of rutting is associated with shear deformation rather than densification. Clearly therefore, shear stress is one of the critical factors affecting pavements performance, hence the serious need to fully comprehend its' characteristics in asphalt pavements. Accordingly, therefore, it is imperative to comprehend the loading and stress induction characteristics. However, most conventional pavement design methodologies assume that tyre pavement contact stress is equivalent to tyre inflation pressure and is uniformly distributed over a circular contact area, a theory which fairly contradicts the actuality. In this Study, analyses of the mode of loading, load impact/intensity and loading characteristics are fastidiously carried out by employing the TACH-MD models presented in Equations 1 ~ 6. Equation 1 defines the correlations between shear stress, τ_{li} load intensity, P_l and pavement thickness, t_p; whilst Equation 2 expresses the same for tyre pressure, σ_{tp} instead of load intensity, P_l. The relation between the maximum shear stress, $\tau_{max.}$ and maximum tyre pressure, $\sigma_{tp,max}$ is delineated in Equation 3, while the location of the maximum shear stress, $d_{p,\tau_{max}}$ is defined in Equation 4. On the other hand, Equations 5 and 6 are adopted in computing the maximum impact and contact stresses for simulating aircraft landing impact and vehicular contact stresses, respectively.

$$\tau_{li} = [-15.78ln(P_l) + 24.964]t_p^2 - [2.1299ln(P_l) - 3.648]t_p + 0.0786ln(P_l) - 0.092\ (MPa) \quad (1)$$

$$\tau_{tp} = \left[-5.879\sigma_{tp}^2 - 7.7879\sigma_{tp} - 15.769\right]t_p^2 + \left[1.7817exp\left(0.7443\sigma_{tp}\right)\right]t_p + 0.094ln\left(\sigma_{tp}\right) + 0.2111\ (MPa) \quad (2)$$

International Journal of Engineering Research & Technology (IJERT)
ISSN: 2278-0181
Vol. 9 Issue 12, December-2020

$$\tau_{max.} = 6 \times 10^{-8}\sigma_{tp,max}^2 + 0.0001\sigma_{tp,max} + 0.1454\ (MPa) \Big\| \sigma_{tp,max}\ in\ kPa \quad (3)$$

$$d_{p,\tau_{max}} = 16.19ln(\tau_{max.}) + 89.674\ (mm) \quad (4)$$

$$\sigma_{mivs} = 0.0113\sigma_{tp}^2 - 14.835\sigma_{tp} + 6065.2\ (kPa) \quad (5)$$

$$\sigma_{mcvs} = 0.007571\sigma_{tp}^2 - 9.93945\sigma_{tp} + 4063.684\ (kPa) \quad (6)$$

Examples of the analytical results generated employing Equations 2, 5 and 6 are provided graphically in Figures 1 ~ 3. Figure 1 depicts the shear stress profile within the upper pavement layers indicating the location and profile of the maximum shear stress.

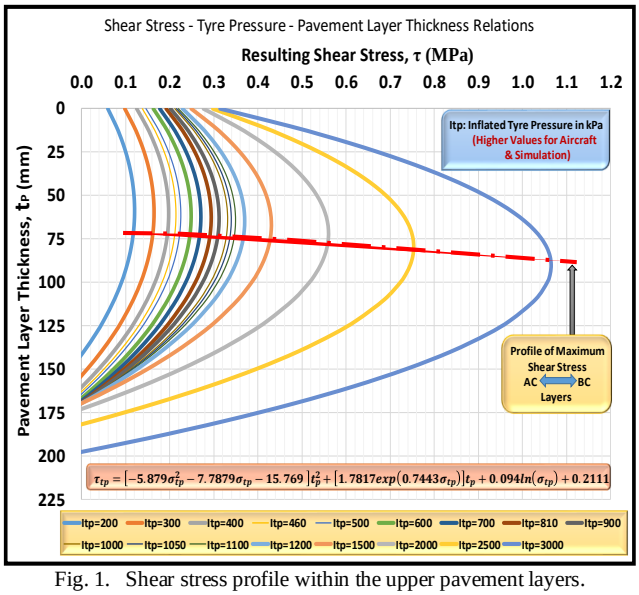

Fig. 1. Shear stress profile within the upper pavement layers.

On the other hand, the influence of the magnitude of the tyre pressure and the initial impact stress on the stress and strain distributions and the resulting profile at varying depths is demonstrated in Figures 2 and 3, respectively. The following derivations can be made from these figures: i) the magnitude and characteristic profiles of the shear stress, vertical stress and vertical strain are dependent upon the contact tyre pressure; ii) the maximum shear stress occurs at approximately $0.5t_p$, where t_p represents the upper pavement thickness; the shear and vertical stress distribution profiles are distinctly different; iii) the magnitude of the impact elastic strain decreases with increased contact stress; and iv) on the contrary, the secant elastic strain limit increases with increased design/impact stress, which is in agreement with the concepts of dynamic loading effects on limiting elastic strain and KHSSS (kinematic hardening soil small strain) models ([2],[3], [4], [5] [6], [7]).

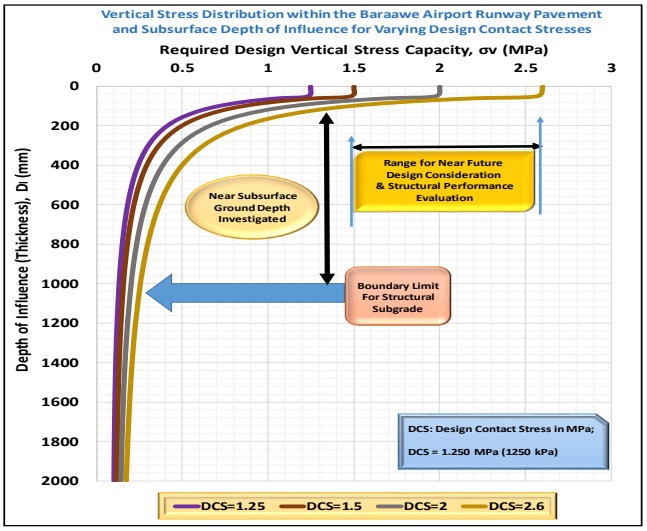

Fig. 2. Vertical stress distribution for varying pavement and subgrade layers.

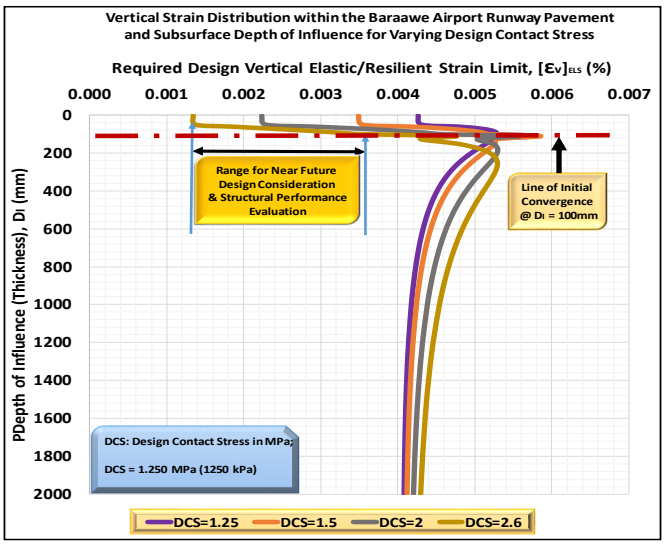

Fig. 3. Vertical strain distribution for varying pavement and subgrade layers.

III. Validation of the Quasi-Mechanistic TACH-MD VDL Analytical Models Proposed/Adopted

A. TACH-MD VDL models for determining progressive deformation

The importance of developing reliable models for characterizing the progressive deformation of foundation ground, pavements and other geo-structures, cannot be overemphasized. The quasi-mechanistic TACH-MD VDL (vibrational dynamic loading) analytical models proposed/adopted in this Study are introduced hereafter. Characterization of progressive vertical (axial) and lateral (horizontal) deformation under sustained vibrational dynamic loading ([1], [6], [8],[9]) is achieved through the application of the models defined in Equations 7 ~ 14.

$$\varepsilon_a = [0.0279exp(0.0937PI)] \times ln(N_{vdA}) - 0.5045exp(0.057PI) \quad (7)$$

$$\varepsilon_{lat.} = \{[0.0279exp(0.0937PI)] \times ln(N_{vdA}) - 0.5045exp(0.057PI)\} \times [0.864 - 0.063ln(E_0)]\| \quad (8)$$

International Journal of Engineering Research & Technology (IJERT)
ISSN: 2278-0181
Vol. 9 Issue 12, December-2020

$$PI_{Res.} = 0.00017778E_0^2 - 0.1654E_0 + 37.726 \| PI \leq 35\% \; and \; E_0 \leq 400MPa \quad (9)$$

$$E_0^{Res.} = E_0^{Initial} exp(-0.0735PI) \quad (10)$$

$$PI_{Res.} = -13.60544ln\frac{E_0^{Res.}}{E_0^{Initial}} \quad (11)$$

Consequently;

$$\varepsilon_a = [0.0279exp(0.0937\langle 0.00017778E_0^2 - 0.1654E_0 + 37.726 \rangle)] \times ln(N_{vdA}) - 0.5045exp(0.057\langle 0.00017778E_0^2 - 0.1654E_0 + 37.726 \rangle) \quad (12)$$

$$\varepsilon_a = \{0.0279exp(\langle 1.6658 \times 10^{-5}E_0^2 - 0.0155E_0 + 3.53493 \rangle)\} \times ln(N_{vdA}) - 0.5045exp\{\langle 4.43346 \times 10^{-5}E_0^2 - 9.4278 \times 10^{-3}E_0 + 2.50382 \rangle\} \quad (13)$$

and,

$$\varepsilon_a = \left\{0.0279exp\left[-1.27483ln\left(\frac{E_0^{Res.}}{E_0^{Initial}}\right)\right]\right\} \times ln(N_{vdA}) - 0.5045exp\left[-0.77551ln\left(\frac{E_0^{Res.}}{E_0^{Initial}}\right)\right] \quad (14)$$

B. Other TACH-MD VDL models adopted

Other quasi-mechanistic TACH-MD VDL analytical models proposed/adopted in this paper are defined in Equations 15 ~ 25.

1) Secant Dynamic Stress - Cumulative Load Cycles - PI Model for Clayey Geomaterials

$$\Delta\sigma_d = [-0.0604P_I^2 + 1.2562P_I + 43.922] \times N_{vd}^{-(-2\times10^{-5}P_I^2 + 0.0008P_I + 0.1208)} \quad (15)$$

$$\Delta\sigma_d = 10.978\varepsilon_a^{-0.612} \; (kPa) \quad (16)$$

$$E_D = 1097.8\varepsilon_a^{-1.612} \; (kPa) \| \quad (17)$$

2) Secant Dynamic – Static Stress Correlations for Clayey Geomaterials

$$[\Delta\sigma_d] = 8.172\sigma_{ucs}^{0.7838} \; (kPa) \quad (18)$$

3) Secant Dynamic – Static Stress Model for Gravely Geomaterials

$$[\Delta\sigma_d] = 12.06\sigma_{ucs}^{0.6304} \; (kPa) \quad (19)$$

4) Secant Dynamic Stress – PI Model for Clayey Geomaterials

$$[\Delta\sigma_d] = 232154P_I^{-2.14} \; (kPa) \quad (20)$$

5) Secant Dynamic Stress – PI Model for Gravely Geomaterials

$$[\Delta\sigma_d] = 75.66P_I^{0.896} \; (kPa) \quad (21)$$

6) Cumulative Dynamic Stress – Strain – PI Universal Model for Clayey Geomaterials

$$\sigma_{cid} = -1 \times 10^{14}P_I^{-9.092}\varepsilon_a^2 + 1.63 \times 10^9P_I^{-5.003}\varepsilon_a + 0.3308P_I^2 - 22.35P_I + 318.05 \; (kPa) \quad (22)$$

7) Cumulative Dynamic Stress – Cumulative Loading Cycles – PI Universal Model for Clayey Geomaterials

$$\sigma_{cid} = (0.3308P_I^2 - 22.35P_I + 318.05)ln(N_{A,DL}) - 6.1788P_I^2 + 231.55P_I - 2315.3 \; (kPa) \quad (23)$$

8) Cumulative Dynamic Stress – Cumulative Loading Cycles – PI Universal Model for Gravelly Geomaterials

$$\sigma_{cid} = \sum_{i=1}^{i\geq1m\;Cycles}\{E_D = 1097.8\varepsilon_a^{-1.612}\} \times \left\{[0.0279exp(0.0937PI)] \times ln(N_{vdA}) - 0.5045exp(0.057PI)\right\} \Big/ 100 \Big\| \quad (24)$$

$$\sigma_{cid} = \sum_{i=1}^{i\geq1m\;Cycles}\{E_D = 1097.8\varepsilon_a^{-1.612}\} \times \left\{[0.0279exp(0.0937PI)] \times ln(N_{vdA}) - 0.5045exp(0.057PI)\right\} \Big/ 100 \Big\| \quad (25)$$

C. Validation of the TACH-MD models

The data that partially validates the TACH-MD models adopted in the characterization, modelling and simulation of vibrational dynamic loading is summarized in Table I.

TABLE I. SUMMARY OF DATA COMPARING MEASURED AND MODELLED DYNAMIC LOADING RESULTS.

S/N	Loading Time (Hrs.)	Loading Time (mins.)	Loading Cycles (No.)	Measured Values: Neat BCS	Measured Values: BCS + 2% Lime	Measured Values: BCS + Con Aid + 2% Lime	Measured Values: BCS + 5% Lime	Predicted Values: Neat BCS	Predicted Values: BCS + 2% Lime	Predicted Values: BCS + Con Aid + 2% Lime	Predicted Values: BCS + 5% Lime
	Loading Sequence			Vertical Deformation, Ɛa (%)							
1	0.017	1	2800	1.15	0.43	0.12	0.1	1.315	0.429	0.564	-0.086
2	0.033	2	5600					1.703	0.672	0.831	0.053
3	0.050	3	8400					1.929	0.814	0.986	0.134
4	0.067	4	11200	2.22	1.21	0.87	0.23	2.090	0.914	1.097	0.191
5	0.083	5	14000					2.215	0.992	1.183	0.236
6	0.167	10	28000					2.603	1.235	1.450	0.374
7	0.250	15	42000	3.16	1.28	1.26	0.27	2.830	1.377	1.605	0.455
8	0.333	20	56000					2.991	1.478	1.716	0.512
9	0.417	25	70000					3.116	1.556	1.802	0.557
10	0.500	30	84000	3.28	1.22	1.59	0.506	3.218	1.620	1.872	0.593
11	0.667	40	112000	3.505	1.25	1.78	0.67	3.379	1.721	1.983	0.651
12	0.833	50	140000					3.503	1.799	2.069	0.695
13	1.000	60	168000					3.605	1.863	2.139	0.732
14	1.167	70	196000					3.692	1.917	2.198	0.762
15	1.333	80	224000					3.766	1.963	2.249	0.789
16	1.5	90	252000					3.832	2.005	2.295	0.813
17	2.0	120	336000	3.83	1.66	2.29	0.69	3.993	2.105	2.405	0.870
18	2.3	137	384000	5.33					2.152	2.457	0.897
19	3.0	180	504000	Neat BCS Failed After 0.364 Cycles	2.01	2.58	0.82		2.247	2.561	0.951
20	4.0	240	672000		2.16	2.57	0.86		2.348	2.672	1.008
21	5.0	300	840000		2.28	2.76	1.37		2.426	2.758	1.053
22	6.0	360	1008000		2.39	2.78	1.41		2.490	2.828	1.089
23	7.0	420	1176000		Testing Terminated after 1Million Cycles				2.544	2.887	1.120
23	19.0	1,140	3192000						2.894	3.271	1.319
24	59.5	3571	9998800						3.294	3.710	1.547

On the other hand, the graphical depictions of the results tabulated in Table I are plotted in Figures 4 and 5 in both

International Journal of Engineering Research & Technology (IJERT)
ISSN: 2278-0181
Vol. 9 Issue 12, December-2020

arithmetic and semi-log scales, respectively. The tabulated data and graphical figures also make a comparison between measured and modelled results. It can be can be noted that, in all cases, an appreciable fitting of the characteristic curves is achieved for the varying natural and stabilized black cotton soils from the Lake Victoria Region of Western Kenya.

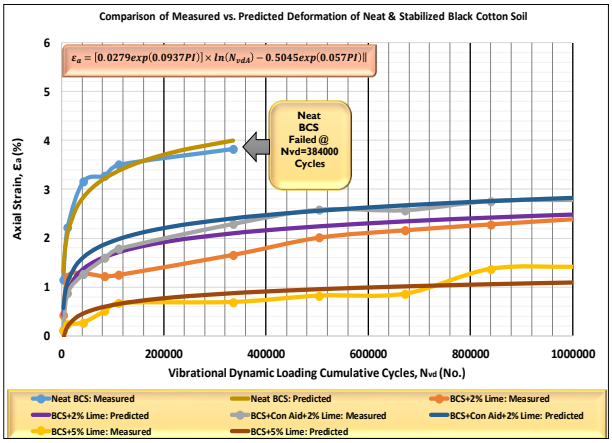

Fig. 4. Comparison of measured and modelled deformation results under dynamic loading (arithmetic scale).

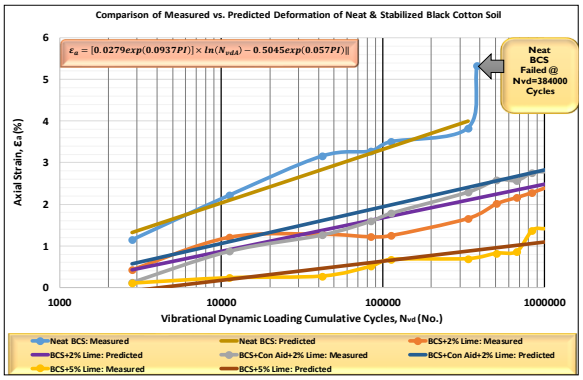

Fig. 5. Comparison of measured and modelled deformation results under dynamic loading (semi-log scale).

Characteristics of the modulus of deformation of natural black cotton soil, Afmadow and Baraawe silty clays (Somalia) are graphically depicted in Figures 6 and 7 for loadings up to 10 million and 1 million cycles, respectively.

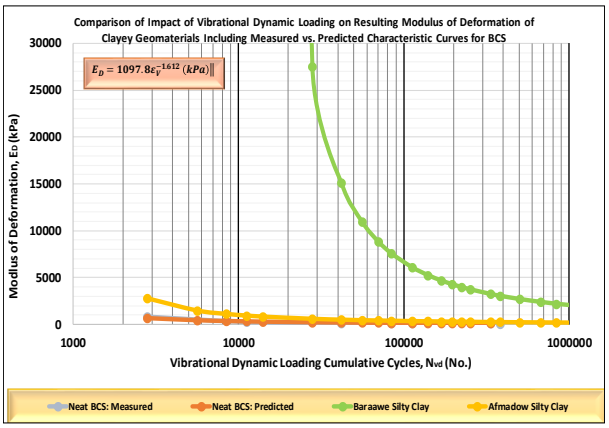

Fig. 6. Comparison of measured and modelled results for impact of dynamic loading on modulus of deformation $[N_{vdl} = 10M]$.

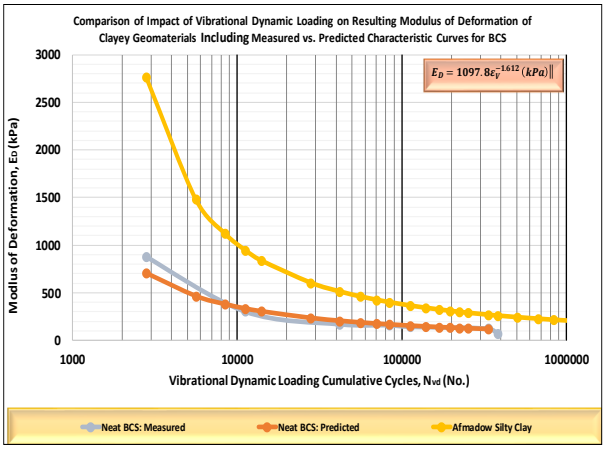

Fig. 7. Comparison of measured and modelled results for impact of dynamic loading on modulus of deformation $[N_{vdl} = 1M]$.

All the depicted graphs also include a comparison of measured and predicted results. It can be observed that, in conformity with their magnitude of initial stiffness, the Baraawe silty clay has the highest resistance to deformation, whilst the BCS registers the lowest. Measured vs. predicted BCS results show quasi-perfect superimposition.

Further validation of the TACH-MD VDL models is udertaken throughout this paper by comparing measured and geo-mathematically modelled results.

IV. Principal Results Adopted for VDL Analyses

A. Example of parametric principal design parameters adopted for VDL analyses

Table II presents a summary of the principal design parameters adopted for dynamic loading analysis undertaken for Bardhere and Diinsoor gravels sampled from Somalia.

TABLE II. Example of Parametric Principal Design Parameters Adopted for Vibrational Dynamic Loading (VDL) Analysis.

Summary of Principal Parameters Adopted for Dynamic Loading Analysis												
Construction Stage →	Pre-Construction						Post-Construction					
Parametric Description ↓	Afmadow			Hudur			Bardhere			Diinsoor		
Gravel Wearing Course (GCW) Bearing Capacity, CBR (%)	45			20			32			14		
Equivalent Base Course (EBC) Bearing Capacity, CBR (%)	To Be Deterined During Design Stage			To Be Deterined During Design Stage			32			14		
Equivalent Sub-Base (ESB) Bearing Capacity, CBR (%)							32			14		
Structural Subgrade Bearing Capacity, CBR (%)	11			20			29			8		
Gravel Wearing Course (GCW) Bearing Capacity, UCS (MPa)	1.087			0.483			0.771			0.338		
Equivalent Base Course (EBC) Bearing Capacity, UCS (MPa)	To Be Deterined During Design Stage			To Be Deterined During Design Stage			0.771			0.338		
Equivalent Sub-Base (ESB) Bearing Capacity, UCS (MPa)							0.771			0.338		
Structural Subgrade Bearing Capacity, UCS (MPa)							0.700			0.193		
Gravel Wearing Course (GCW) Elastic Modulus, Eo (Mpa)	232			95			147			72		
Equivalent Base Course (EBC) Elastic Modulus, Eo (Mpa)	To Be Deterined During Design Stage			To Be Deterined During Design Stage			147			72		
Equivalent Sub-Base (ESB) Elastic Modulus, Eo (Mpa)							147			72		
Structural Subgrade Resilient Modulus, MR (MPa)	58			95			133			44		
Mean Pavement Thickness Determined from DCP Tests, t_{dcp} (mm)	To Be Deterined During Design Stage			To Be Deterined During Design Stage			263			205		
Computational Models Adopted →	Values Computed Based on Conventional SN/CBR Models						Values Computed Based on Quasi-Mechanistic Models					
Structural Layer Designation	GWC	EBC	ESB	GWC	EBC	ESB	GWC	EBC	ESB	GWC	EBC	ESB
Computed Discrete Structural Layer Thickness, tstr. (mm)	To Be Deterined During Design Stage			To Be Deterined During Design Stage			107	62	94	100	48	57
Existing Modulus Ratio (mm/MPa)							0.728	0.422	0.639	1.389	0.667	0.792
Required Discrete Structural Layer Stiffness, Eo (MPa) [To Achieve a PBBD (Performance Based Balanced Design)]							4573	4573	491	3953	3953	1188
Required Full Depth Composite Pavement Stiffness, Eo (MPa) [To Achieve a PBBD (Performance Based Balanced Design)]							1365			1365		
Existing Full Depth (Composite) Structural Thickness, T_{FD} (mm)							263			205		
Example of Computed Values for Enhanced Structural Capacity Required for Fokker50 as Design Aircraft for Bardhere & Diinsoor Airstrips												
Computational Models Adopted →	Values Computed Based on Conventional SN/CBR Models						Values Computed Based on Quasi-Mechanistic Models					
Allowable Full Depth (Composite) Pavement Thickness, T_{FD} (mm)	To Be Deterined During Design Stage			To Be Deterined During Design Stage			300			420		
Required Full Depth (Composite) Pavement Thickness, T_{FD} (mm)							300			450		
Structural Layer Designation	GWC	EBC	ESB	GWC	EBC	ESB	GWC	EBC	ESB	GWC	EBC	ESB
Computed Discrete Structural Layer Thickness, tstr. (mm)	To Be Deterined During Design Stage			To Be Deterined During Design Stage			100	100	100	150	150	150
Existing Modulus Ratio (mm/MPa)							0.022	0.035	0.216	0.057	0.119	0.325
Required Discrete Structural Layer Stiffness, Eo (MPa) [To Achieve a PBBD (Performance Based Balanced Design)]							4573	2835	462	2635	1265	462
Required Full Depth Composite Pavement Stiffness, Eo (MPa) [To Achieve a PBBD (Performance Based Balanced Design)]							853			853		
Legend: SE-Structural Evaluation; GWC-Gravel Wearing Course; EBC-Equivalent Base Course; ESF: Equivalent Structural Foundation												

International Journal of Engineering Research & Technology (IJERT)
ISSN: 2278-0181
Vol. 9 Issue 12, December-2020

B. Summary of results adopted for analyses of VDL impact

Summaries of the results adopted for analyses of vibrational dynamic loading impact are tabulated in Tables III ~ V for natural clayey geomaterials and Tables VI ~ VIII for natural gravelly geomaterials.

TABLE III. SUMMARY OF DATA ADOPTED FOR ANALYSIS OF DYNAMIC LOADING EFFECTS ON DEFORMATION CHARACTERISTICS OF CLAYEY GEOMATERIALS.

Dynamic Loading Effects on Deformation & Modulus of Deformation Characteristics of Clayey Geomaterials								
Loading Cycles (No.)	Neat BCS: Measured	Neat BCS: Predicted	Neat Baraawe Silty Clay	Neat Afmadow Expansive Clay	Neat BCS: Predicted from Measured Values	Neat BCS: Predicted	Neat Baraawe Silty Clay	Neat Afmadow Expansive Clay
	Vertical Deformation, Ɛa (%)				Resulting Modulus of Deformation, E_o (kPa)			
2800	1.15	1.315		0.564	876	706		2764
5600		1.703		0.831		466		1481
8400		1.929		0.986		381		1122
11200	2.22	2.090		1.097	304	334		945
14000		2.215	0.031	1.183		305	295015	837
28000		2.603	0.136	1.450		235	27510	603
42000	3.16	2.830	0.197	1.605	172	205	15102	512
56000		2.991	0.240	1.716		188	10954	460
70000		3.116	0.274	1.802		176	8867	425
84000	3.28	3.218	0.301	1.872	162	167	7600	400
112000	3.505	3.379	0.344	1.983	145	154	6118	364
140000		3.503	0.378	2.069		145	5265	340
168000		3.605	0.406	2.139		139	4702	322
196000		3.692	0.429	2.198		134	4299	308
224000		3.766	0.449	2.249		129	3992	297
252000		3.832	0.467	2.295		126	3750	288
336000	3.83	3.993	0.510	2.405	126	118	3250	267
383600	5.33	4.068	0.530	2.457	74	114	3054	258
504000		4.220	0.571	2.561		108	2708	241
672000		4.381	0.614	2.672		101	2407	225
840000		4.506	0.648	2.758		97	2209	214
1008000		4.608	0.676	2.828		94	2066	205
1176000		4.694	0.699	2.887		91	1956	199
3192000		5.253	0.849	3.271		76	1429	162
9998800		5.892	1.021	3.710		63	1061	133

TABLE IV. SUMMARY OF DATA ADOPTED FOR ANALYSIS OF DECAY STRESS CHARACTERISTICS OF CLAYEY GEOMATERIALS SUBJECTED TO VIBRATIONAL DYNAMIC LOADING EFFECTS.

Dynamic Loading Effects on Stress-Strain Characteristics of Clayey Geomaterials								
Loading Cycles (No.)	Neat BCS: Measured	Neat BCS: Predicted	Neat Baraawe Silty Clay	Neat Afmadow Expansive Clay	Neat BCS: Predicted from Measured Values	Neat BCS: Predicted	Neat Baraawe Silty Clay	Neat Afmadow Expansive Clay
	Strain, Ɛa (%)				Resulting Deviatoric Stress, Δσ (kPa)			
2800	1.15	1.315		0.564	10.08	9.29		15.59
5600		1.703		0.831		7.93		12.30
8400		1.929		0.986		7.34		11.07
11200	2.22	2.090		1.097	6.74	6.99		10.37
14000		2.215	0.031	1.183		6.75	91.80	9.91
28000		2.603	0.136	1.450		6.11	37.29	8.75
42000	3.16	2.830	0.197	1.605	5.43	5.81	29.70	8.22
56000		2.991	0.240	1.716		5.61	26.29	7.89
70000		3.116	0.274	1.802		5.48	24.26	7.66
84000	3.28	3.218	0.301	1.872	5.31	5.37	22.88	7.48
112000	3.505	3.379	0.344	1.983	5.10	5.21	21.08	7.22
140000		3.503	0.378	2.069		5.10	19.91	7.04
168000		3.605	0.406	2.139		5.01	19.07	6.89
196000		3.692	0.429	2.198		4.94	18.43	6.78
224000		3.766	0.449	2.249		4.88	17.92	6.68
252000		3.832	0.467	2.295		4.82	17.50	6.60
336000	3.83	3.993	0.510	2.405	4.83	4.70	16.58	6.42
383600	5.33	4.068	0.530	2.457	3.94	4.65	16.19	6.33
504000		4.220	0.571	2.561		4.55	15.47	6.17
672000		4.381	0.614	2.672		4.45	14.79	6.02
840000		4.506	0.648	2.758		4.37	14.32	5.90
1008000		4.608	0.676	2.828		4.31	13.96	5.81
1176000		4.694	0.699	2.887		4.26	13.67	5.74
3192000		5.253	0.849	3.271		3.98	12.13	5.32
9998800		5.892	1.021	3.710		3.71	10.84	4.92
			Equivalent Dynamic Strength (kPa)			135.6	474	193
			Static Strength, UCS (kPa)			36.2	169	48.3
					CBR (%)	1.5	7	2

TABLE V. SUMMARY OF DATA ADOPTED FOR ANALYSIS OF CUMULATIVE STRESS-STRAIN CHARACTERISTICS OF CLAYEY GEOMATERIALS SUBJECTED TO VIBRATIONAL DYNAMIC LOADING .

Summary of Dynamic Loading Effects on Stress-Strain Characteristics of Clayey Geomaterials								
Loading Cycles (No.)	Neat BCS: Measured	Neat BCS: Predicted	Neat Baraawe Silty Clay	Neat Afmadow Expansive Clay	Neat BCS: Predicted from Measured Values	Neat BCS: Predicted	Neat Baraawe Silty Clay	Neat Afmadow Expansive Clay
	Strain, Ɛa (%)				Resulting Deviatoric Stress, Δσ (kPa)			
2800	1.15	1.315		0.564	10.08	9		16
5600		1.703		0.831		17		28
8400		1.929		0.986		25		39
11200	2.22	2.090		1.097	6.74	32		49
14000		2.215	0.031	1.183		38	92	59
28000		2.603	0.136	1.450		44	129	68
42000	3.16	2.830	0.197	1.605	5.43	50	159	76
56000		2.991	0.240	1.716		56	185	84
70000		3.116	0.274	1.802		61	209	92
84000	3.28	3.218	0.301	1.872	5.31	67	232	99
112000	3.505	3.379	0.344	1.983	5.10	72	253	106
140000		3.503	0.378	2.069		77	273	113
168000		3.605	0.406	2.139		82	292	120
196000		3.692	0.429	2.198		87	311	127
224000		3.766	0.449	2.249		92	329	134
252000		3.832	0.467	2.295		97	346	140
336000	3.83	3.993	0.510	2.405	4.83	101	363	147
383600	5.33	4.068	0.530	2.457	3.94	106	379	153
504000		4.220	0.571	2.561		111	394	159
672000		4.381	0.614	2.672		115	409	165
840000		4.506	0.648	2.758		119	423	171
1008000		4.608	0.676	2.828		124	437	177
1176000		4.694	0.699	2.887		128	451	183
3192000		5.253	0.849	3.271		132	463	188
9998800		5.892	1.021	3.710		136	474	193
			Equivalent Dynamic Strength (kPa)			135.6	474.1	193.1
			Static Strength, UCS (kPa)			36.2	169	48.3
					CBR (%)	1.5	7	2

TABLE VI. SUMMARY OF DATA ADOPTED FOR ANALYSIS OF MODULUS OF DEFORMATION CHARACTERISTICS OF GRAVELLY GEOMATERIALS SUBJECTED TO VIBRATIONAL DYNAMIC LOADING.

Dynamic Loading Effects on Axial Strain & Modulus of Deformation Characteristics of Somalia Gravel Geomaterials														
Loading Cycles (No.)	Hudur Gravel	Afmadow Gravel	Bardhere Gravel		Diinsoor Gravel		Baraawe Silty Clay	Hudur Gravel	Afmadow Gravel	Bardhere Gravel		Diinsoor Gravel		Baraawe Silty Clay
	Vertical Deformation, Ɛa (%)							Resulting Modulus of Deformation, E_o (MPa)						
			Post-Construct	Pre-Construct	Pre-Construct	Post-Construct				Post-Construct	Pre-Construct	Pre-Construct	Post-Construct	
2800														
5600														
8400														
11200														
14000							0.031							295
28000							0.136							28
42000							0.197							15
56000							0.240							11
70000							0.274							9
84000						0.011	0.301						1569	8
112000						0.038	0.344						212	6
140000			0.018		-0.074	0.059	0.378			720			105	5
168000			0.034		-0.063	0.076	0.406			261			69	4.7
196000		0.005	0.047		-0.053	0.091	0.429		5527	153			52	4.3
224000		0.015	0.058		-0.044	0.104	0.449		917	107			42	4.0
252000		0.025	0.068		-0.036	0.115	0.467		433	83			36	3.8
336000	0.014	0.047	0.093		-0.018	0.142	0.510	1064	153	50			26	3.3
383600	0.023	0.057	0.104		-0.009	0.154	0.530	465	111	42			22	3.1
504000	0.043	0.078	0.128		0.009	0.180	0.571	176	67	30		2297	17	2.7
672000	0.063	0.101	0.153		0.027	0.207	0.614	94	45	23		363	14	2.4
840000	0.079	0.118	0.172	0.009	0.042	0.228	0.648	65	35	19	2029	183	12	2.2
1008000	0.092	0.132	0.187	0.020	0.054	0.245	0.676	51	29	16	593	123	11	2.1
1176000	0.103	0.144	0.201	0.029	0.064	0.260	0.699	43	25	15	326	93	10	2.0
3192000	0.174	0.221	0.286	0.088	0.128	0.354	0.849	18	12	8	55	30	6	1.4
9998800	0.256	0.310	0.385	0.156	0.202	0.462	1.021	10	7	5	22	14	4	1.1

International Journal of Engineering Research & Technology (IJERT)
ISSN: 2278-0181
Vol. 9 Issue 12, December-2020

TABLE VII. SUMMARY OF DATA ADOPTED FOR ANALYSIS OF SECANT STRESS DECAY CHARACTERISTICS OF GRAVELLY GEOMATERIALS SUBJECTED TO VIBRATIONAL DYNAMIC LOADING.

Dynamic Loading Effects on Deformation Characteristics of Somalia Gravel Geomaterials														
Loading Cycles (No.)	Hudur Gravel	Afmadow Gravel	Bardhere Gravel		Diinsoor Gravel		Baraawe Silty Clay	Hudur Gravel	Afmadow Gravel	Bardhere Gravel		Diinsoor Gravel		Baraawe Silty Clay
	Vertical Deformation, εa (%)							Resulting Secant Deviatoric Stress, Δσ (kPa)						
			Post-Construct	Pre-Construct	Pre-Construct	Post-Construct				Post-Construct	Pre-Construct	Pre-Construct	Post-Construct	
2800														
5600														
8400														
11200														
14000							0.031							91.80
28000							0.136							37.29
42000							0.197							29.70
56000							0.240							26.29
70000							0.274							24.26
84000						0.011	0.301						173.14	22.88
112000						0.038	0.344						81.01	21.08
140000			0.018			0.059	0.378			128.80			61.91	19.91
168000			0.034			0.076	0.406			87.66			52.97	19.07
196000		0.005	0.047			0.091	0.429		279.24	71.51			47.61	18.43
224000		0.015	0.058			0.104	0.449		141.19	62.54			43.98	17.92
252000		0.025	0.068			0.115	0.467		106.19	56.70			41.32	17.50
336000	0.014	0.047	0.093			0.142	0.510	149.39	71.49	46.94			36.28	16.58
383600	0.023	0.057	0.104		0.009	0.154	0.530	109.07	63.32	43.74		196.26	34.46	16.19
504000	0.043	0.078	0.128		0.009	0.180	0.571	75.40	52.22	38.65		200.09	31.35	15.47
672000	0.063	0.101	0.153	0.004	0.027	0.207	0.614	59.38	44.79	34.69	334.24	99.30	28.77	14.79
840000	0.079	0.118	0.172	0.009	0.042	0.228	0.648	51.78	40.64	32.26	190.87	76.59	27.12	14.32
1008000	0.092	0.132	0.187	0.020	0.054	0.245	0.676	47.20	37.92	30.59	119.68	65.77	25.94	13.96
1176000	0.103	0.144	0.201	0.029	0.064	0.260	0.699	44.06	35.96	29.34	95.29	59.24	25.04	13.67
3192000	0.174	0.221	0.286	0.088	0.128	0.354	0.849	31.97	27.64	23.60	48.51	38.56	20.72	12.13
9998800	0.256	0.310	0.385	0.156	0.202	0.462	1.021	25.29	22.49	19.70	34.27	29.18	17.61	10.84
			Equivalent Dynamic Strength (kPa)					594	923	707	823	765	749	474
			Static Strength, UCS (kPa)					483	1086	627	1070	852	701	169
							CBR (%)	20	45	26	44	35	29	7
							Plasticity Index, PI (%)	10	11	12	8	9	13	18

TABLE VIII. SUMMARY OF DATA ADOPTED FOR ANALYSIS OF CUMULATIVE STRESS-STRAIN CHARACTERISTICS OF GRAVELLY GEOMATERIALS SUBJECTED TO VIBRATIONAL DYNAMIC LOADING.

Cumulative Stress-Strain Characteristics Under Vibrational Dynamic Loading: Effects on Deformation Characteristics of Somalia Gravel Geomaterials														
Loading Cycles (No.)	Hudur Gravel	Afmadow Gravel	Bardhere Gravel		Diinsoor Gravel		Baraawe Silty Clay	Hudur Gravel	Afmadow Gravel	Bardhere Gravel		Diinsoor Gravel		Baraawe Silty Clay
	Vertical Deformation, εa (%)							Resulting Secant Deviatoric Stress, Δσ (kPa)						
			Post-Construct	Pre-Construct	Pre-Construct	Post-Construct				Post-Construct	Pre-Construct	Pre-Construct	Post-Construct	
2800														
5600														
8400														
11200														
14000							0.031							92
28000							0.136							129
42000							0.197							159
56000							0.240							185
70000							0.274							209
84000						0.011	0.301					173		232
112000						0.038	0.344					254		253
140000			0.018			0.059	0.378			129		316		273
168000			0.034			0.076	0.406			216		369		292
196000		0.005	0.047			0.091	0.429		279	288		417		311
224000		0.015	0.058			0.104	0.449		420	351		461		329
252000		0.025	0.068			0.115	0.467		527	407		502		346
336000	0.014	0.047	0.093			0.142	0.510	149	598	454		538		363
383600	0.023	0.057	0.104		0.009	0.154	0.530	258	661	498		573		379
504000	0.043	0.078	0.128		0.009	0.180	0.571	334	714	537		604		394
672000	0.063	0.101	0.153	0.004	0.027	0.207	0.614	393	758	571		633		409
840000	0.079	0.118	0.172	0.009	0.042	0.228	0.648	445	799	603		660		423
1008000	0.092	0.132	0.187	0.020	0.054	0.245	0.676	492	837	634		686		437
1176000	0.103	0.144	0.201	0.029	0.064	0.260	0.699	536	873	663		711		451
3192000	0.174	0.221	0.286	0.088	0.128	0.354	0.849	568	901	687		732		463
9998800	0.256	0.310	0.385	0.156	0.202	0.462	1.021	594	923	707		749		474
			Equivalent Dynamic Strength (kPa)					594	923	707	823	765	749	474
			Static Strength, UCS (kPa)					483	1086	627	1070	852	701	169
							CBR (%)	20	45	26	44	35	29	7
							Plasticity Index, PI (%)	10	11	12	8	9	13	18

V. VDL CHARACTERISTICS OF CLAYEY GEOMATERIALS

Simulation of the Afmadow silty clay foundation ground is undertaken by comparatively evaluating the dynamic loading characteristics of clayey subgrade geomaterials. This involves the comparative analysis of: i) load impact (maximum impact upon contact) characteristics depicting the effects of lime stabilization on black cotton soil (BC) subjected to vibrational dynamic loading; ii) dynamic loading impact on the modulus of deformation of non-stabilized clayey geomaterials; iii) decay characteristics of secant stress as a result of cumulative dynamic loading effects; iv) deformation characteristics of clayey geomaterials under dynamic loading; and, v) cumulative stress-strain characteristics of neat clayey geomaterials subjected to vibrational dynamic loading.

A. Analysis of load impact characteristics of natural and hydraulically stabilized clayey geomaterials

A summary of the results of the impact of vibrational dynamic loading (VDL) on the characteristics of natural, lime and lime-conaid treated black cotton soil (BCS) and natural Afmadow silty clay is presented in Table IX, whilst the corresponding deformation characteristics are graphically depicted in Figures 8 and 9 for VD loadings within the range of 10 million and 1 million cycles, respectively.

The characteristic curves in these graphs show that: i) notwithstanding the geomaterial type, deformation is significantly impacted by the cumulative cycles of the VDL; ii) in conformity with their bearing strengths (CBRs), the Baraawe silty clay quantitatively exhibits the lowest deformation, whilst the BCS registers the highest (4 days soaked CBRs: Baraawe=7%; Afmadow=2% BCS=1.5%); ii) lime stabilization enhances deformation resistance of the BCS; and iii) the Afmadow silty clay subgrade requires in-situ ground improvement.

TABLE IX. COMPARISON OF NATURAL AND STABILIZED CLAYEY GEOMATERIALS SUBJECTED TO VIBRATIONAL DYNAMIC LOADING RESULTS.

Comparison of Vibrational Dynamic Loading Effects on Deformation Characteristics of Clayey Geomaterials								
Loading Cycles (No.)	Neat BCS: Measured	Neat BCS: Predicted	Neat Baraawe Silty Clay	Neat Afmadow Expansive Clay	Neat BCS: Predicted from Measured Values	Neat BCS: Predicted	Neat Baraawe Silty Clay	Neat Afmadow Expansive Clay
	Vertical Deformation, εa (%)				Resulting Modulus of Deformation, E_D (kPa)			
2800	1.15	1.315		0.564	876	706		2764
5600		1.703		0.831		466		1481
8400		1.929		0.986		381		1122
11200	2.22	2.090		1.097	304	334		945
14000		2.215	0.031	1.183		305	295015	837
28000		2.603	0.136	1.450		235	27510	603
42000	3.16	2.830	0.197	1.605	172	205	15102	512
56000		2.991	0.240	1.716		188	10954	460
70000		3.116	0.274	1.802		176	8867	425
84000	3.28	3.218	0.301	1.872	162	167	7600	400
112000	3.505	3.379	0.344	1.983	145	154	6118	364
140000		3.503	0.378	2.069		145	5265	340
168000		3.605	0.406	2.139		139	4702	322
196000		3.692	0.429	2.198		134	4299	308
224000		3.766	0.449	2.249		129	3992	297
252000		3.832	0.467	2.295		126	3750	288
336000	3.83	3.993	0.510	2.405	126	118	3250	267
383600	5.33	4.068	0.530	2.457	74	114	3054	258
504000		4.220	0.571	2.561		108	2708	241
672000		4.381	0.614	2.672		101	2407	225
840000		4.506	0.648	2.758		97	2209	214
1008000		4.608	0.676	2.828		94	2066	205
1176000		4.694	0.699	2.887		91	1956	199
3192000		5.253	0.849	3.271		76	1429	162
9998800		5.892	1.021	3.710		63	1061	133

International Journal of Engineering Research & Technology (IJERT)
ISSN: 2278-0181
Vol. 9 Issue 12, December-2020

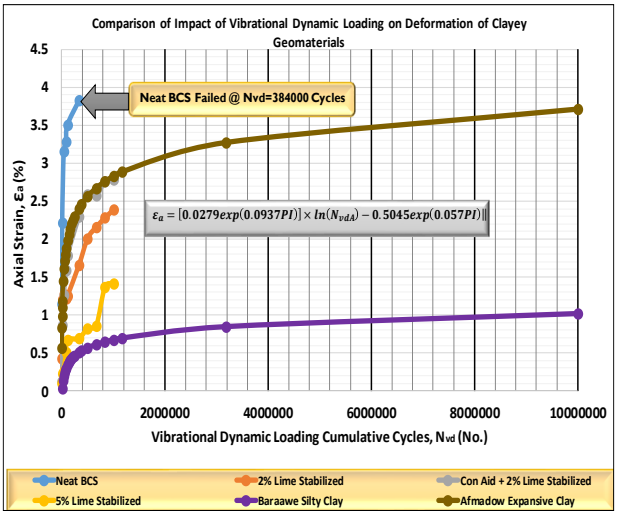

Fig. 8. Comparison of impact of dynamic loading on natural and stabilized clays $[N_{vdl} = 10M]$.

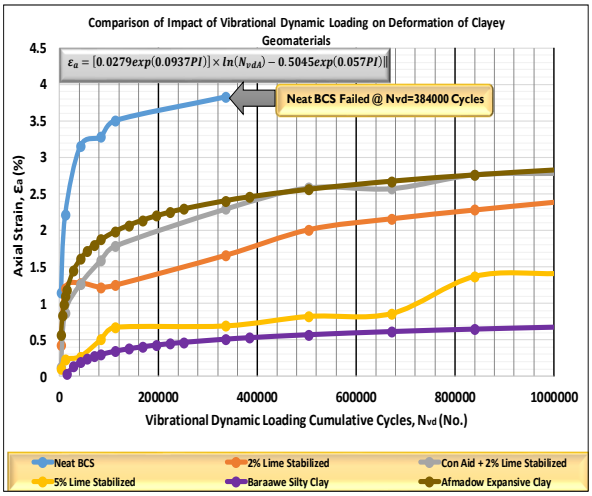

Fig. 9. Comparison of impact of dynamic loading on natural and stabilized clays $[N_{vdl} = 1M]$.

B. Analysis of secant stress decay resulting from cumulative dynamic load impact on natural clayey geomaterials

Modelled decay characteristics of the secant deviator stress of natural black cotton soil, Afmadow silty clay and Baraawe silty clay are graphically depicted in Figure 10 for loadings up to 1 million with comparison to measured data.

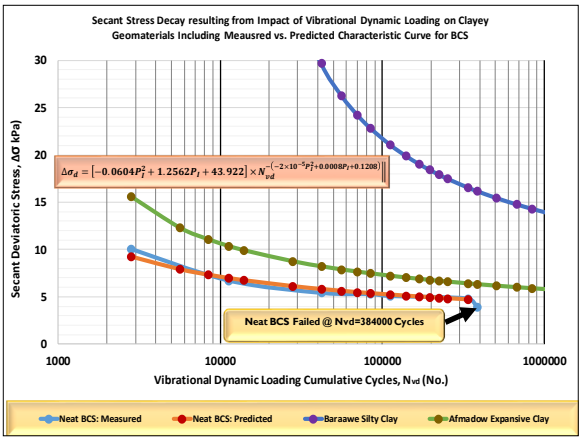

Fig. 10. Decay characteristics of secant deviator stress under dynamic loading $[N_{vdl} = 10M]$.

The results in Figure 10 show that: i) the mode and rate of secant deviatoric stress decay as a result of cumulative VDL is dependent upon the nature and stiffness of the clayey geomaterial; and ii) a very good agreement exists between the measured and modelled (predicted) results.

Figure 11 depicts the superimposed VDL stress-strain curves for varying clays. The graph also includes a comparison of measured and predicted results for BCS. As was deduced form Figure 10, the Baraawe silty clay has the highest resistance to stress decay, whilst the BCS registers the lowest. Measured vs. predicted BCS results show quasi-perfect superimposition.

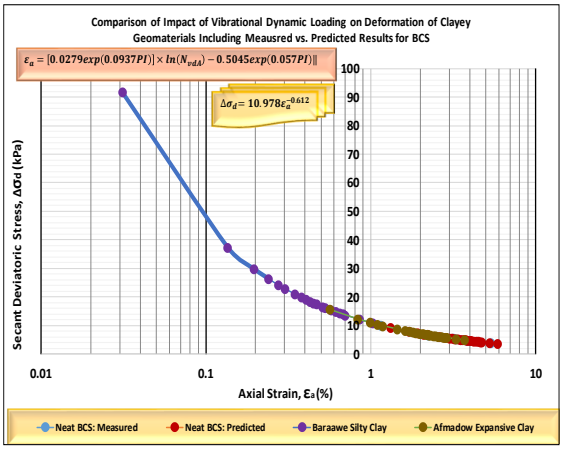

Fig. 11. Stress-strain characteristics under dynamic loading $[N_{vdl} = 10M]$.

C. Deformation characteristics of natural clayey geomaterials subjected to VDL

Deformation characteristics under dynamic loading of natural black cotton soil, Afmadow silty clay and Baraawe silty clay are graphically depicted in Figures 12 and 13 for loadings up to 3.2 million and 100,000 (one hundred thousand) cycles, respectively; with a comparison of measured and predicted results for BCS. The results from these figures clearly indicate that: i) deformation, defined in terms of axial (vertical) strain is significantly influenced by the nature and stiffness of the clayey geomaterials; and ii) the impact of VDL is more intense within the initial phase of loading tending to a residual state with increased cumulative loading (Figure 13).

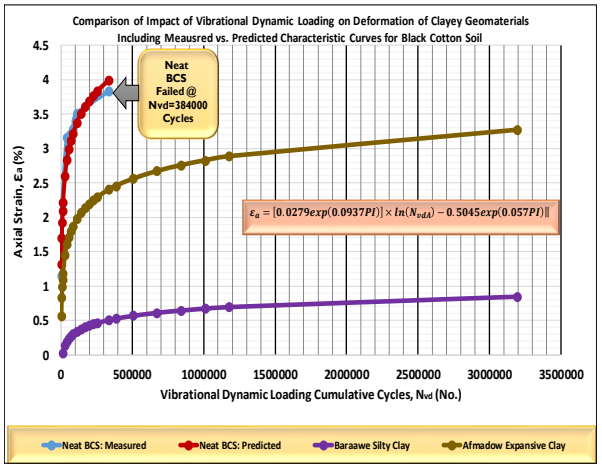

Fig. 12. Deformation characteristics of clays under dynamic loading $[N_{vdl} = 3.2M]$.

International Journal of Engineering Research & Technology (IJERT)
ISSN: 2278-0181
Vol. 9 Issue 12, December-2020

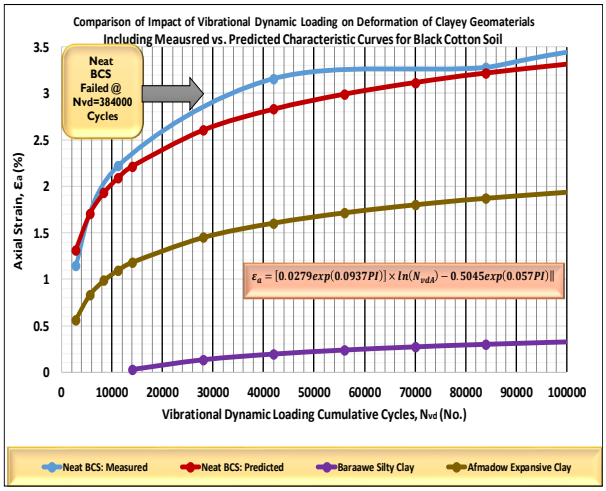

Fig. 13. Deformation characteristics of clays under dynamic loading $[N_{vdl} = 100000]$.

D. Analysis of cumulative stress-strain characteristics of natural clayey geomaterials subjected to VDL

The influence of dynamic loading on cumulative impact stress, σ_{cid} for $[max.N_{vdl} = 3.2M]$ is depicted in Figure 14 for natural Baraawe and Afmadow silty clays as well as natural black cotton soil (BCS). It can be observed that the Baraawe silty clay exhibits the highest impact stress; a state that is attributable to its lower plasticity index and higher stiffness (4 days soaked resilient moduli in $MPa: Baraawe = 39; Afmadow = 12\, BCS = 9$).

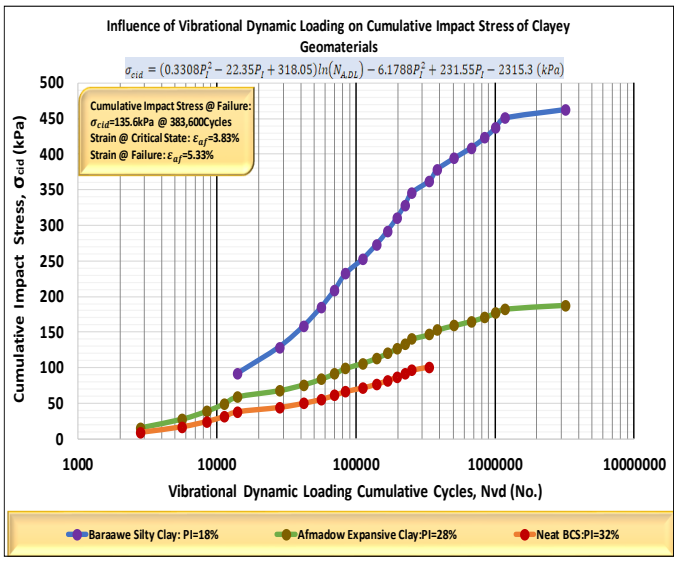

Fig. 14. Influence of dynamic loading on cumulative impact stress $[Max.N_{vdl} = 3.2M]$.

On the other hand, the characteristics of the cumulative impact stress plotted against axial strain under vibrational dynamic loading are depicted in Figure 15. The results in these figures show that: i) the Afmadow silty clay subgrade requires ground improvement to enhance its resistance to impact stress and reduce the magnitude of deformation; and, ii) black cotton soil (BCS) exhibits the highest deformation strain due to its lower resistance to impact stress [lower stiffness (deformation resistance)].

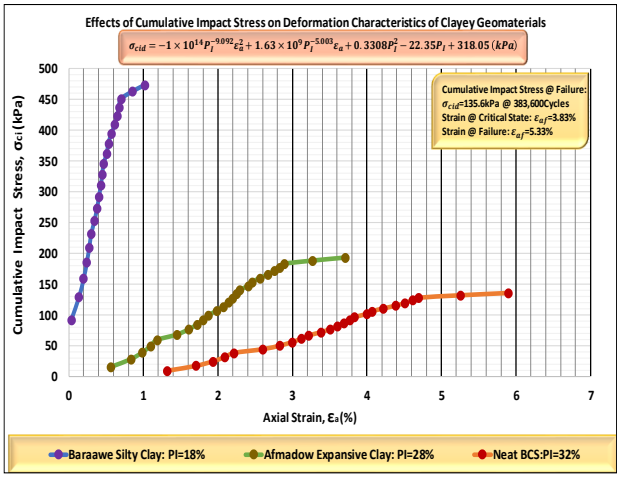

Fig. 15. Cumulative impact stress-strain characteristics under dynamic loading.

❑ *Implication of results from this Section V: Simulation of foundation/subgrade ground characteristics for design*

1. *Vibrational dynamic loading (VDL) has distinctly significant impact on the geotechnical engineering properties, characteristics and geotechnical quantities of clayey subgrade geomaterials.*
2. *As the dynamic loading increases, the deformation and impact stress resistance of the clayey subgrade geomaterials reduces exponentially with the most drastic reduction exhibited within the initial (primary) phase of loading.*
3. *The Afmadow silty clay subgrade requires in-situ ground improvement preferably using ND (Non-Destructive) GI techniques and/or replacement.*
4. *Designs based on comprehensive subgrade geomaterials and in-situ ground property analysis as well as high standards of QCA are imperative in ensuring achievement of Performance Based Value Engineering (PB-VE) pavement structures.*
5. *Both Afmadow and Hudur gravels require OPMC (Optimum Mechanical & Chemical) stabilization in order to achieve the geotechnical engineering properties required for the design & construction specifications for the designated design aircraft.*

VI. VDL EFFECTS ON GRAVELLY GEOMATERIALS

The effects of vibrational dynamic loading on the characteristics of gravelly geomaterials are analyzed in this Section VI. Essentially, this involves the analysis of: i) dynamic loading impact on the modulus of deformation of non-stabilized gravelly geomaterials; ii) decay characteristics of secant stress as a result of cumulative dynamic loading effects; iii) deformation characteristics of gravelly geomaterials under dynamic loading; and, v) cumulative stress-strain characteristics of neat gravelly geomaterials subjected to vibrational dynamic loading.

A. Analysis of VDL impact on modulus of deformation and axial strain of gravelly geomaterials: Comparative simulation of pre- and post-conctruction charatceristics

Simulated Pre-Construction (PrC) and Post-Construction (PoC) characteristics of the modulus of deformation and cumulative strain subjected to VDL on some typical Somalia gravels are graphically depicted and compared in Figures 16 and 17 for cumulative loadings of up to 10 million cycles.

International Journal of Engineering Research & Technology (IJERT)
ISSN: 2278-0181
Vol. 9 Issue 12, December-2020

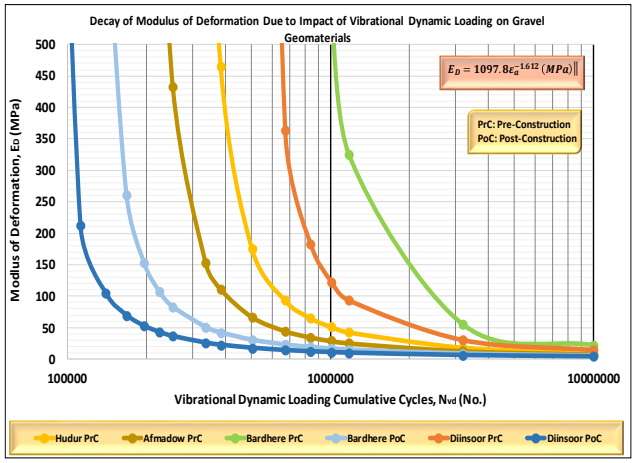

Fig. 16. Impact of dynamic loading on modulus of deformation of gravels $[Max.N_{vdl} = 10M]$.

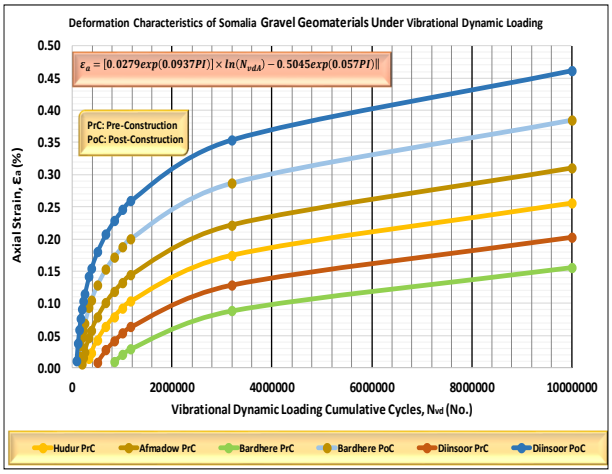

Fig. 17. Cumulative strain characteristics of gravels under dynamic loading $[Max.N_{vdl} = 10M]$.

It can be observed and derived, from Figures 16 and 17 that: i) the rate of decay of the modulus of deformation is more drastic for the post-construction gravels implying that effects of reconstitution/remolding are visibly apparent and that these geomaterials may have been in varying degrees of weathered states culminating in the increase in fines contents, which implies loss in bearing capacity and stiffness; ii) resistance to deformation under dynamic loading is dependent on the magnitude of both plasticity index and the bearing strengths; iii) the mode of decay is influenced by both the magitude of the initial stiffness and number of cumulative loading cycles, whereas the charcteristic curves in Figure 17 show that the axial deformation (straining) is almost entirely dependent only on the initial stiffness; and iv) both stiffness dacay and straining are more acute within the initial stage of loading. Refer to Tables VII and VIII for further data correlation and verification.

B. Analysis of cumulative deviator stress decay resulting from cumulative VDL impact on gravelly geomaterials

Decay characteristics of the secant deviator stress of some typical Somalia gravels are graphically depicted in Figure 18 for loadings of up to 10 million cumulative cycles. That drastic deviator stress decay occurs within the zone of initial loading can very well be observed from this figure.

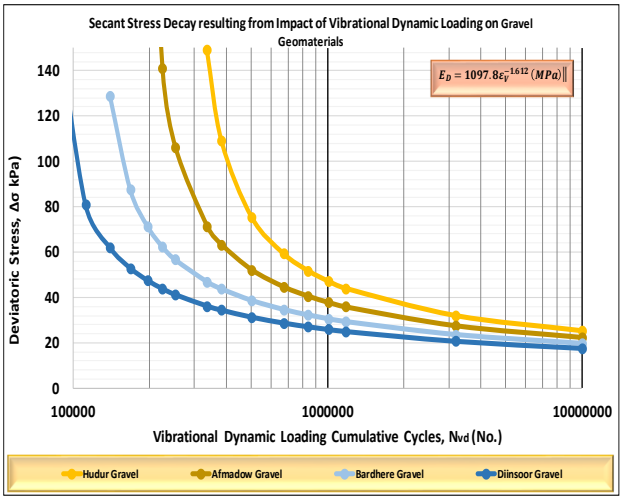

Fig. 18. Deviator stress decay characteristics of gravels under dynamic loading $[Max.N_{vdl} = 10M]$.

C. Influence of VDL and axial strain level on the cumulative impact stress of gravelly geomaterials

The influence of cumulative VDL on the cumulative impact stress is demonstrated in Figure 19, whilst its strain level dependency is depicted in Figure 20 for loadings of up to 10 million cumulative cycles. In both cases it can be observed that the cumulative impact stress increases with both cumulative loading and straining tending towards a residual state after approximately one million (1,000,000) loading cycles. However, it can be inferred that, whereas the threshold for the initiation of the residual state tendency is virtually clearly defined at this level, that of cumulative deformation occurs at varying strain levels depending on the magnitude of the initial stiffness, plasticity index as well as compressive and bearing strength (refer to Tables VII and VIII).

It can further be derived that reconstitution/remolding reduces the levels/thresholds of both cumulative loading and deformation resistance of the cumulative impact stress (compare Pre-Construction (PrC) and Post-Construction (PoC) characteristic curves in Figures 19 and 20).

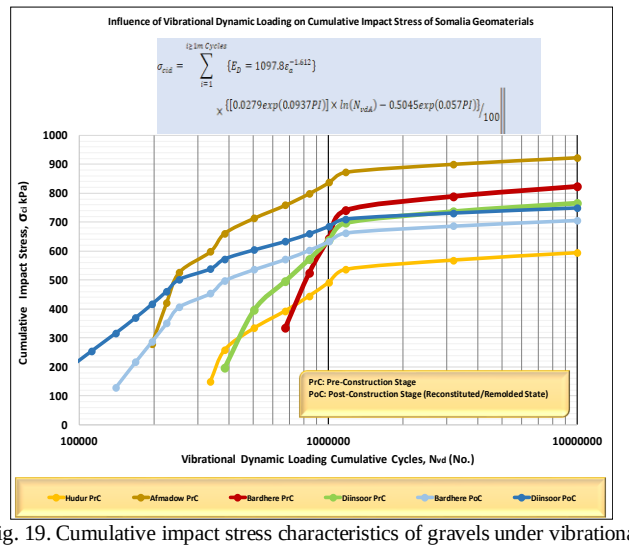

Fig. 19. Cumulative impact stress characteristics of gravels under vibrational dynamic loading.

International Journal of Engineering Research & Technology (IJERT)
ISSN: 2278-0181
Vol. 9 Issue 12, December-2020

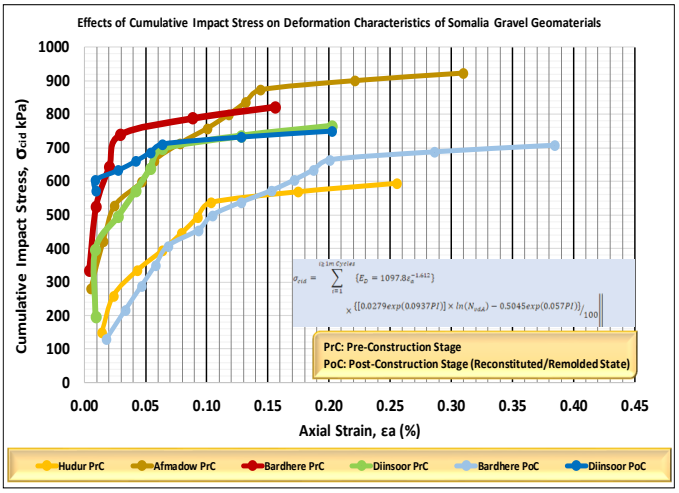

Fig. 20. Cumulative impact stress-strain characteristics of gravels under vibrational dynamic loading.

❑ *Implication of results in this Section VI: Stress-strain and deformation resistance (geotechnical engineering) characteristics for design.*

1. Vibrational dynamic loading has distinctly significant impact on the geotechnical engineering properties, characteristics and geotechnical quantities of the gravelly geomaterials designated for use in pavement construction.
2. As the dynamic loading increases, the deformation and impact stress resistance of the gravelly geomaterials reduces exponentially with the most drastic reduction exhibited within the initial (primary) phase of loading.
3. Both Afmadow and Hudur gravels require mechanical as well as chemical stabilization in order to meet design and construction specification requirements.
4. Designs based on comprehensive pavement geomaterials analysis of the effects of vibrational dynamic loading in retrospect to the maintenance of high standards of QCA are imperative in ensuring achievement of Performance Based Value Engineering (PB-VE) pavement structures.
5. Both Afmadow and Hudur gravels require OPMC stabilization in order to achieve the geotechnical engineering properties required for design & construction specifications of the designated design aircraft.

VII. Analysis of Stiffness Decay and Deformation of Typical Somalia Gravels Under Cumulative VDL

A. *Decay and deformation characteristics*

The impact of vibrational dynamic loading on the decay characteristics of secant modulus of deformation and the strain deformation of Somalia gravels is depicted in Figures 21 and 22, respectively; for VDLs of up to 30 million cumulative cycles. It can be deduced that both the stiffness decay and straining deformation resistance largely depend on the magnitude of the initial stiffness (elastic modulus).

The results in these figures further make a comparison of the Pre-Construction and Post-Construction characteristics, which show that the Pre-Construction (PrC) Bardhere gravel with the highest initial elastic modulus $[E_0 = 133MPa]$ exhibits the highest resistance to deformation (note that the maximum strain for this gravel is; $[\varepsilon_a]_{max} = 1.8\%$.

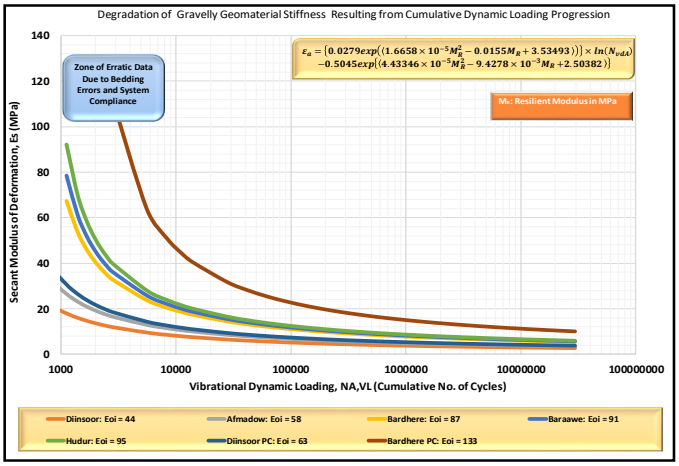

Fig. 21. Impact of vibrational dynamic loading on secant modulus of deformation of Somalia gravels $[Max.N_{vdl} = 30M]$.

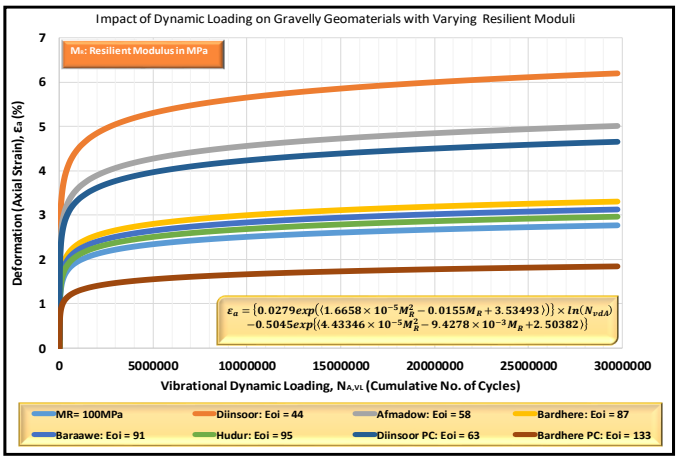

Fig. 22. Deformation characteristics of Somalia gravels under dynamic loading [$N_{vdl} = 30M$].

B. *Analysis of VDL impact on modulusof deformation within the initial phase of loading*

The characteristic curves depicting stiffness degradation resulting from progressive cumulative vibrational dynamic loading within the initial phase of loading $[1000 \leq N_{vdl} \leq 100000\ cycles]$ are graphically plotted in Figure 23.

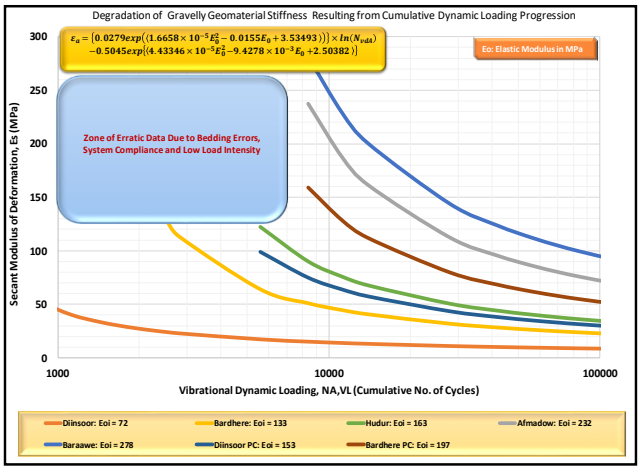

Fig. 23. Modulus of deformation decay characteristics Somalia gravels under dynamic loading $[1000 \leq N_{vdl} \leq 100000]$.

International Journal of Engineering Research & Technology (IJERT)
ISSN: 2278-0181
Vol. 9 Issue 12, December-2020

The following observations and/or derivations can be made from the modelled results graphically plotted in Figure 23: i) there exists a zone of erratic data (within the region of very small strains), the causes of which may be attributable to bedding errors, system compliance and low load intensity (limitation of transducer resolution); ii) it can be explicitly confirmed that the mode and magnitude of impact of VDL is predominantly dependent upon the initial stffness of the geomaterial; iii) application of the TACH-MD VDL models, which were developed within a mechanistic-empirical framework based on experimental testing data, is limited within this zone; and iv) the limiting factor, which is the number of cumulative load cycles, depends on the magnitude of the initial stiffness with geomaterials of higher stiffness registering higher cyclic limits possibly due to the fact that bedding error correction requires higher load intensity for stiffer specimens.

❑ *Implication of Results in this Section VII: Simulation of pavement gravel characteristics within initial phase of VDL for design and construction*

1. *Deformation resistance is predominantly dependent upon the magnitudes of the initial/original stiffness (elastic modulus) and the plasticity characteristics.*
2. *Vibrational dynamic loading has distinctly significant impact on the geotechnical engineering properties, characteristics and geotechnical quantities of the gravelly geomaterials designated for use in pavement construction.*
3. *As the dynamic loading increases, the deformation and impact stress resistance of the gravelly geomaterials reduces exponentially with the most drastic reduction exhibited within the initial (primary) phase of loading.*
4. *Further research is required in order to determine a sustainable solution to the data collection and processing within the erratic zone which occurs within the region of very small strains (initial phase of the vibrational dynamic loading* $[N_{vdl} < 10000 cycles]$.
5. *Both Afmadow and Hudur gravels require OPMC stabilization in order to achieve the geotechnical engineering properties required for design & construction specifications of the ATR72 design aircraft.*
6. *It is crucially vital to consider the adverse effects of bedding errors, system compliance, low load intensity (limitation of transducer resolution) and environmental factors (Sec. IX) during VDL testing.*

VIII. Analysis of Cumulative Stress-Strain Characteristics of Clays and Gravels Under Progressive VDL

Under this Section VIII, cumulative stress-strain characteristics of specimens subjected to dynamic loading are analyzed. The analysis includes evaluation of the effects of reconstitution/remolding, which are outlined under several preceding sub-Sections. This is achieved by comparing Pre-Construction (PrC) and Post-Construtution (PoC) results.

A. Cumulative impact stress-strain characteristics of clayey geomaterials

Figure 24 shows the impact of vibrational dynamic loading on cumulative impact stress of clays subjected to dynamic loading $[N_{vdl} = 3.2\ Million\ cycles]$. It can be noted that clayey geomaterials with lower plasticity indices (PIs) exhibit higher cumulative impact stresses and that the Afmadow silty clay subgrade certainly requires ground improvement.

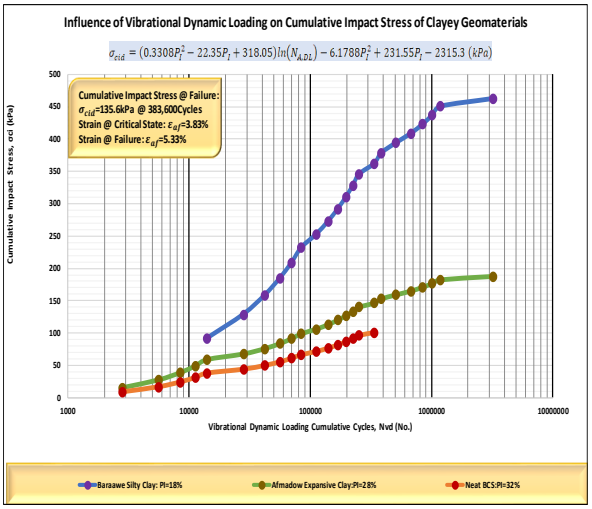

Fig. 24. Impact of dynamic loading on cumulative impact stress of Clays $[N_{vdl} = 3.2M]$.

The characteristics of the cumulative impact stress versus strain of clayey geomaterials are graphically depicted in Figure 25. It can be noted that the Baraawe silty clay with the lowest PI exhibits the highest resistance to deformation.

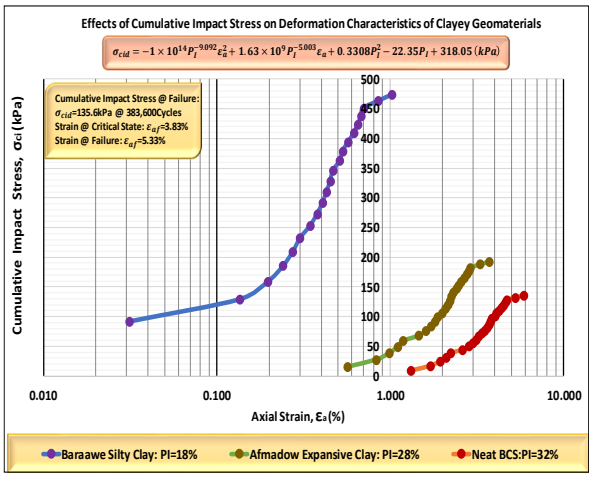

Fig. 25. Cumulative impact stress-strain characteristics of clays under dynamic loading.

B. Cumulative impact stress-strain characteristics of gravelly geomaterials

The impact of VDL on cumulative impact stress of gravels is graphically demonstrated in Figure 26 for loadings of up to $[N_{vdl} = 10\ Million\ cycles]$. It can be noted that gravelly geomaterials with higher strengths and stiffness exhibit higher cumulative impact stresses (refer to results tabulated in Tables VII & VII in Section IV). It can further be observed that the influence of cumulative VDL on the impact stress is more pronounced within the loading zone of 100,000 ~ 1000,000 (one hundred thousand to one million) cycles, after which practically all modelled curves tend to a residual state with increased loading. On the other hand, the characteristics of the cumulative impact stress versus strain for gravels are depicted in Figure 27. It can be noted that the gravels with lower PIs and higher strengths and stiffness (elastic moduli) exhibit the highest resistance to deformation (refer to summary results in Tables VII & VII in Section IV).

International Journal of Engineering Research & Technology (IJERT)
ISSN: 2278-0181
Vol. 9 Issue 12, December-2020

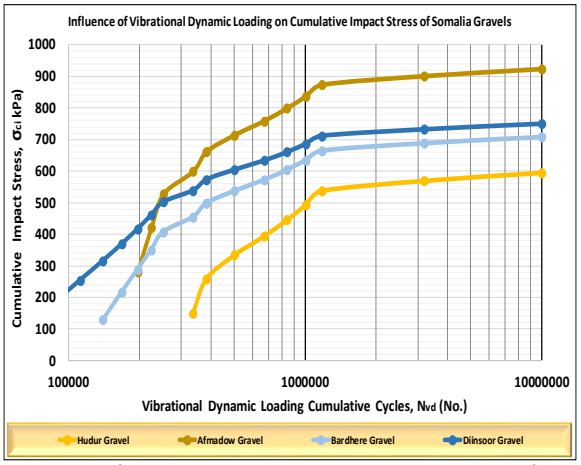

Fig. 26. Impact of dynamic loading on cumulative impact stress of Somalia gravels $[N_{vdl} = 10M]$.

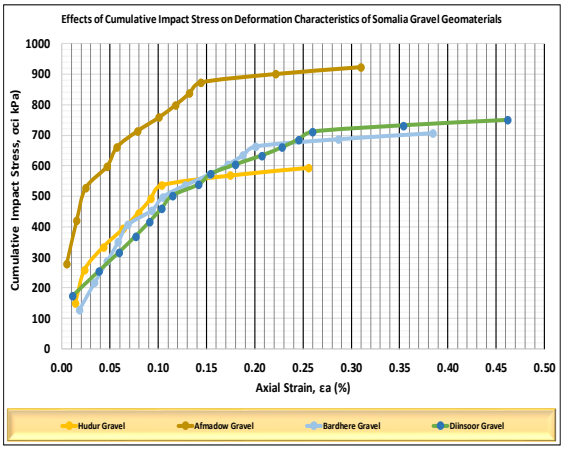

Fig. 27. Cumulative stress-strain characteristics of Somalia gravels under vibrational dynamic loading.

C. Cumulative impact stress-strain characteristics of typical Somalia gravels under VDL: Effects of reconstitution/remolding

The effects of reconstitution/remolding are analyzed through the comparison of the Pre-Construction (PrC) and Post-Construction (PoC) results shown in Figures 28 and 29.

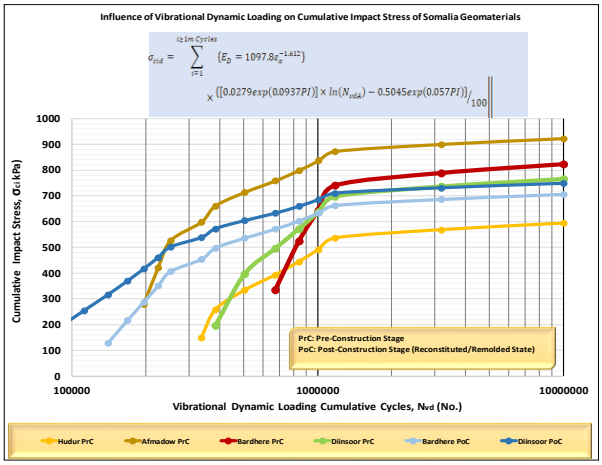

Fig. 28. Impact of dynamic loading on cumulative impact stress of gravels $[N_{vdl} = 10M]$: Comparison of Pre-Construction (PrC) and Post-construction (PoC) characteristics

Figure 28 and the correlation between cumulative impact stress and cumulative progressive strain depicted in Figure 29 clearly show that reconstitution of the gravelly geomaterials reduces strength/stiffness and that the magnitude of this reduction is dependent upon the original strength, stiffness and plasticity index (refer to summary Tables VII & VII in Section IV).

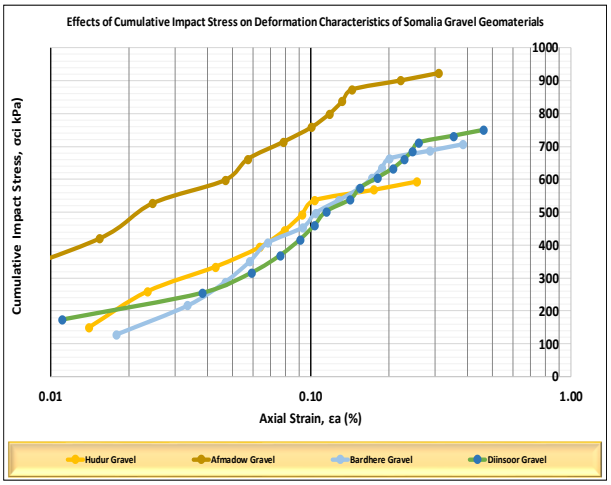

Fig. 29. Cumulative impact stress-strain of Somalia gravels: LS $[N_{vdl} = 10M]$: Comparison of Pre-Construction (PrC) and Post-construction (PoC) characteristics

On the other hand, Figures 30 and 31 show the impact of progressive loading on the magnitude of axial strain (deformation) graphically plotted both in arithmetic and semi-log scale for clarity of comparison of this VDL impact on Pre-Construction (PrC) and Post-construction (PoC) characteristics simulating the effects of reconstitution/remolding and to enable proper analysis thereof.

It can also be inferred from these figures that: i) reconstitution reduces the deformation resistance of gravelly geomaterials; and ii) the magnitude of resistance is proportional to the magnitude of the initial stiffness.

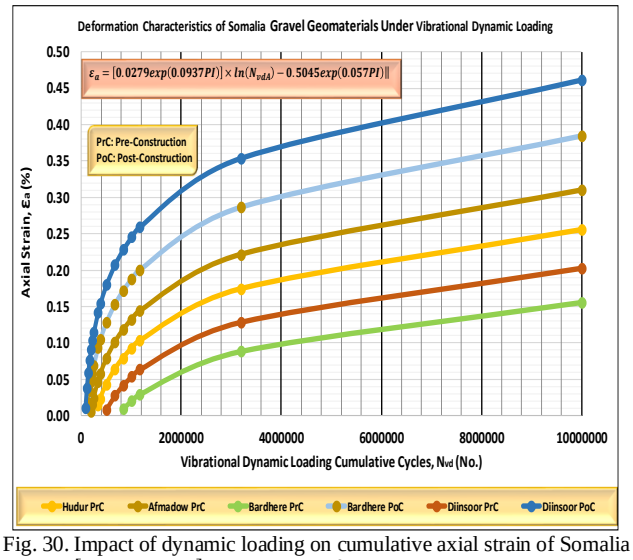

Fig. 30. Impact of dynamic loading on cumulative axial strain of Somalia gravels $[N_{vdl} = 10M]$: Comparison of Pre-Construction (PrC) and Post-construction (PoC) characteristics.

International Journal of Engineering Research & Technology (IJERT)
ISSN: 2278-0181
Vol. 9 Issue 12, December-2020

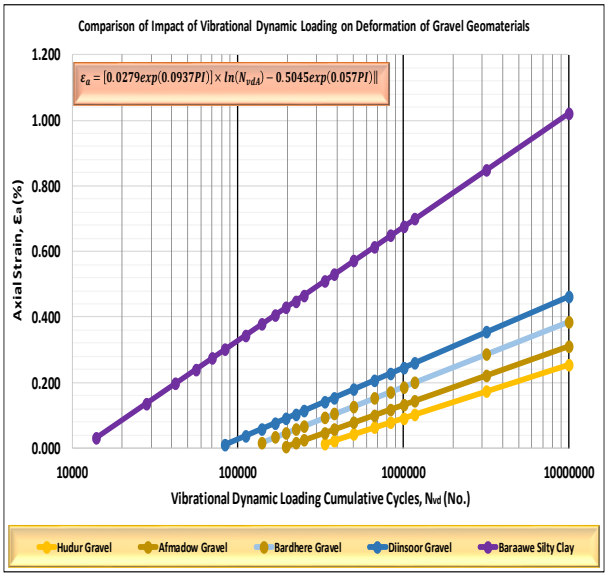

Fig. 31. Impact of dynamic loading on cumulative axial strain of Somalia gravels [$N_{vdl} = 10M$]: Log Scale (LS): Comparison of Pre-Construction (PrC) and Post-construction (PoC) characteristics.

❑ *Implication of Results in Section VIII: Simulation of pavement gravel characteristics subjected to VDL*

1. *Reconstitution/remolding impacts adversely on the geotechnical engineering properties of gravelly geomaterials by reducing strength and deformation resistance (stiffness) making the geomaterials more susceptible to the impact of dynamic loading.*
2. *Deformation resistance is predominantly dependent upon the magnitudes of the initial/original stiffness (elastic modulus) and the plasticity characteristics, particularly under dynamic loading.*
3. *Vibrational dynamic loading has distinctly significant impact on the geotechnical engineering properties, characteristics and geotechnical quantities of the gravelly geomaterials designated for use in pavement construction.*
4. *It is imperative to carry out further comprehensive analyses of the vibrational dynamic loading characteristics during the design stage in order to generate appropriate design parameters.*

IX. Performance Evaluation of VDL Effects

Structural performance simulation of subgrade and pavement geomaterials as well as discrete layers and composite pavement subjected to the effects of vibrational dynamic loading is to be carried out in [10] mainly in consideration of extreme changes in environmental conditions and factors in retrospect to the limiting design parameters.

Based on the prevailing climatic conditions in Afmadow and Hudur, locations of the aerodromes to be designed in Somalia, it was deemed imperative that moisture ~ suction variation be analyzed for both suction and dilatancy characteristics under dynamic loading conditions; the comprehensive testing regime of which is included in the testing matrix, modules defining basic protocols and main testing procedure presented in Section 4.6 of Chapter 4 of [1].

One of the main influencing factors with regard to the impact of moisture ~ suction variation is the PI (plasticity index); refer to [10] for the functional and applicable models as well as validation and comprehensive analytical discussions. An introductory example of influence of PI and correlation with mode of loading (dynamic – static) is subsequently provided.

A. Influence of moisture-suction variation

As can be observed from Figures 32 and 33, plasticity index and mechanical stability (particle size and distribution) have significant influence on both static and dynamic strengths of clayey geomaterials as well as gravels.

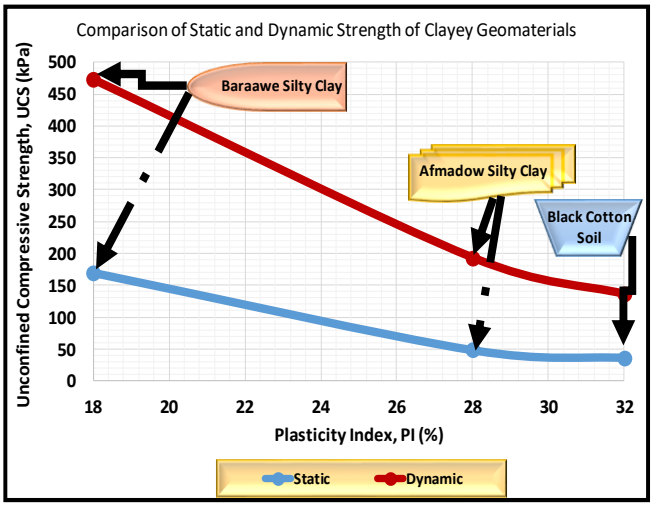

Fig. 32. Impact plasticity index on static and dynamic strengths of clayey geomaterials.

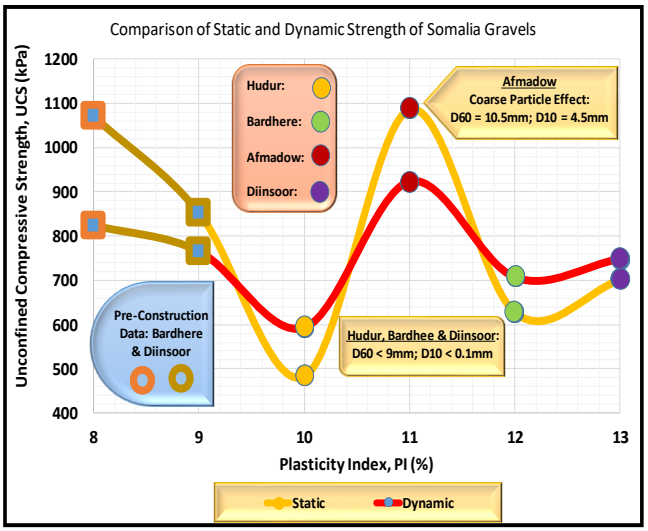

Fig. 33. Impact plasticity index on static and dynamic strengths of Somalia gravels: Without consideration of particle size effect

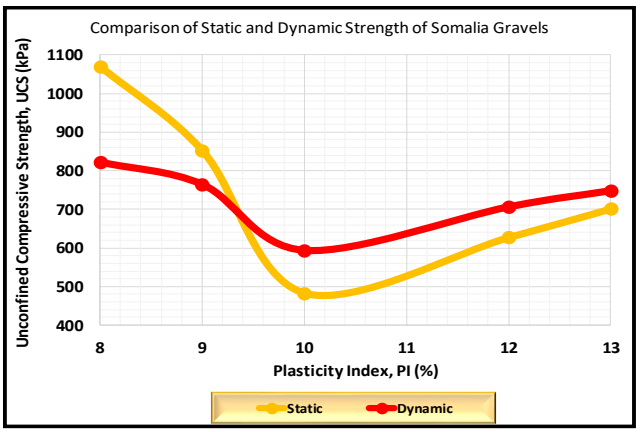

Fig. 34. Impact plasticity index on static and dynamic strengths of Somalia gravels: Corrected particle size effect.

International Journal of Engineering Research & Technology (IJERT)
ISSN: 2278-0181
Vol. 9 Issue 12, December-2020

It can also be noted from these figures that, in general, the dynamic strengths are higher than static strengths for geomaterials with strengths lower than 700kPa ($q_u \leq 700kPa$). It can also be noted that whereas both static and dynamic strengths (UCS) reduce consistently for clayey geomaterials (Figure 32), the characteristic curves in Figure 33 are rather sinusoidal. This is attributable to the effect of mechanical stability (particle size – fines content) as indicated in Figure 33. This fact is verified in Figure 34, which depicts the characteristic curves corrected for particle size effects.

Simulation is therefore carried out, in [10], taking the effects of plasticity index, particle size, mechanical stability, agglomeration, among other factors, into account.

B. Overall performance evaluation

The overall structural performance evaluation of discrete layers and composite pavements is undertaken in [10].

X. CONCLUSIONS

Introduction of sophisticated quasi-mechanistic TACH-MD VDL (vibrational dynamic loading) analytical models, which are useful in carrying out comprehensive analyses of the impact of VDL for purposes of detailed design of highway and aerodrome pavements, has been made in this paper. it has further been demonstrated that the proposed analytical models equipped with a variety of application modules, the validity, lucidity and rationality of which has been explicitly demonstrated, are uniquely functional and effectively applicable for the designated objectives. The following conclusions are derived from the analytical discussions presented in this paper.

1. Vibrational dynamic loading has distinctly significant impact on the geotechnical engineering properties, characteristics and geotechnical quantities of clayey subgrade and gravelly geomaterials for pavements.
2. As the dynamic loading increases, the deformation and impact stress resistance of the clayey and gravelly geomaterials reduces exponentially with the most drastic reduction exhibited within the initial (primary) phase of loading.
3. Designs based on comprehensive subgrade geomaterials, in-situ ground property and pavement geomaterials analyses of the effects of vibrational dynamic loading in retrospect to the maintenance of high standards of QCA are imperative in ensuring achievement of Performance Based Value Engineering (PB-VE) pavement structures.
4. Deformation resistance is predominantly dependent upon the magnitudes of the initial/original stiffness (elastic modulus) and the plasticity characteristics.
5. Reconstitution/remolding impacts adversely on the geotechnical engineering properties of gravelly geomaterials by reducing strength and deformation resistance (stiffness) making the geomaterials more susceptible to the impact of dynamic loading and environmental conditions/factors.
6. Deformation resistance is predominantly dependent upon the magnitudes of the initial/original stiffness (elastic modulus) and the plasticity characteristics, particularly under vibrational dynamic loading.
7. It is imperative to carry out further comprehensive analyses of the vibrational dynamic loading characteristics during the design stage in order to generate appropriate design parameters.

ACKNOWLEDGMENT

The author wishes to acknowledge, with utmost gratitude, the Japan International Cooperation Agency and Kajima Corporation (JICA) for substantially funding the initial stage of this research, the Materials Testing & Research Division (MTRD), Ministry of Transport, Infrastructure, Housing & Urban Development in Kenya, the University of Nairobi and Norconsult for carrying out the initial phase of testing as well as the Research Teams of Kensetsu Kaihatsu Engineering Consultants Limited and the Kenya Geotechnical Society (KGS) for their relentless efforts in providing the due assistance that culminated in the successful compilation of this paper.

REFERENCES

[1] Mukabi, J.N. & Sirmoi, F.W. "Comprehensive Geomaterials Characterization for Design of Aerodrome Pavement Structures:Geotechnical Engineering Report", March 2019. Technical Report No. MFCR-AH-SOM01.

[2] Wichtmann, T., & Trantafyllidis, Th. "Influence of a Cyclic and dynamic Loading History on Dynamic Properties of Dry Sand, Part I: Cyclic and Dynamic Torsional Prestraining, Journal of Soil Dynamics and Earthquake Engineering.

[3] Enomoto, T., Qureshi, O.H., Sato, T., and Koseki, J. "Strength and Deformation Characteristics and Small Strain Properties of Undisturbed Gravelly Soils", Japanese Geotechnical Society, Soils and Foundations 2013, 53(6): pp. 951 – 965.

[4] Gabrys, K., Wojciech, S. & Sobol, E. "Dynamic and Cyclic Static Loading Behavior of Silty-Sandy Clay at Small and Moderate Strains", Acta Sci. Pol. Architectura; 15(4) 2016: pp. 43 – 55.

[5] Mukabi, J.N. "Characterization of consolidation stress-strain-time histories on the pre-failure behavior of natural clayey geomaterials, Proceedings of the VIth International Symosium on Deformation Characteristics on Geomaterials, Buenos Aires, 2015.

[6] Mukabi, J.N. "Unique Analytical Models for Deriving Fundamental Quasi-Mechanistic Design Parameters for Highway and Airport Pavements:, International Journal of Engineering Research & Technology, Vol. 5 Issue 09, September-2016, pp. 61 – 77.

[7] Mukabi, J.N. & Wekesa, S.F. "Case examples of successful application of a new PB-VE design approach for runway pavements in East Africa", Proceedings of the World Road Congress Workshop on Airfields, Seoul, South Korea, CD ROM; November 2015.

[8] Mukabi, J.N. & Hossain, Z. "Characterization and Modeling of Various Aspects of Pre-failure Deformation of Clayey Geomaterials – Fundamental Theories and Analyses", First International Conference on Geotechnique, Construction Materials and Environment GEOMAT, Mie, Japan, November, 2011.

[9] Mukabi, J.N. "Characterization and Modeling of Various Aspects of Pre-failure Deformation of Clayey Geomaterials – Application of Models", First International Conference on Geotechnique, Construction Materials and Environment GEOMAT, Mie, Japan, November, 2011.

[10] Mukabi, J.N. "Comprehensive Quasi-Mechanistic Analytical Approach for Evaluating Structural Performance of Highway and Aerodrome Pavements Under Vibrational Dynamic Loading", unpublished.

[11] US Army Engineer Waterways Experimental Station, Corps of Engineers. "A Procedure for Determining Elastic Moduli of Soils by Field Vibratory Techniques, Miscellaneous Paper No. 4-577; June, 1963.